Desalination and Water Treatment
www.deswater.com

doi: 10.1080/19443994.2015.1049959

57 (2016) 12385–12395
June

Taylor & Francis
Taylor & Francis Group

Biosorption of fluoride from drinking water using spent mushroom compost biochar coated with aluminum hydroxide

Gui-jie Chen[a], Chuan-yi Peng[a], Jiang-yu Fang[b], Yang-yang Dong[a], Xiao-hui Zhu[a], Hui-mei Cai[a,*]

[a]*State Key Laboratory of Tea Plant Biology and Utilization, School of Tea & Food Science and Technology, Anhui Agricultural University, Hefei 230036, Anhui, P.R. China, emails: chenguijie890915@126.com (G.-j. Chen), pcy0917@ahau.edu.cn (C.-y. Peng), dyyhjj@126.com (Y.-y. Dong), 724982105@qq.com (X.-h. Zhu), Tel. +86 551 65786401; Fax: +86 551 65786765; email: hml20@sina.com (H.-m. Cai)*
[b]*College of Life and Environment Science, Huangshan University, Huangshan 245041, Anhui, P.R. China, email: fjy@hsu.edu.cn*

Received 20 September 2014; Accepted 4 May 2015

ABSTRACT

A low-cost and highly efficient biosorbent for the removal of fluoride from drinking water from spent mushroom compost (SMC) that was carbonized (spent mushroom compost biochar, SMCB) coated by aluminum hydroxide. Adsorption studies were performed to investigate the influence of adsorbent dosage, initial fluoride concentration, contact time, pH, and coexisting ions on fluoride adsorption. The fluoride adsorption capacity of the coated SMCB was greater than that of uncoated SMCB. Fluoride adsorption by coated SMCB followed the Langmuir isotherm model, and the maximum adsorption capacity was 36.5 mg/g. The fluoride concentration could be reduced to below 1 mg/L from an initial fluoride concentration of 10 mg/L. While the pH of the solution did play an important role in the fluoride removal capacity, with the SMCB performed well under a wide pH range, from 6.0 to 8.0. These findings indicate that fluoride can effectively be removed from drinking water using modified mushroom cultivation waste biomass.

Key words: Spent mushroom compost (SMC); Fluoride; Adsorption; Aluminum hydroxide; Drinking water

---

1. Introduction

Fluoride is an important trace element and has significant biological roles in organisms. For example, fluoride is essential in the human body to prevent dental and skeletal problems [1]. The United States and Canada began adding fluoride to public water supplies to prevent cavities beginning in 1945 and 1946, respectively [2]. However, excessive ingestion of fluoride leads to serious adverse effects, such as bone cancer and fluorosis [3]. The effective modulation of fluoride in the human body is thus of significant importance. Fluoride enters the human body mainly through drinking water, industrial exposure, food, cosmetics, and drugs, among which drinking water is considered the principal source of daily intake [4]. The recommended concentration of fluoride in water resources, as stipulated by the World Health Organization, is in the range of 0.5–1.5 mg/L [5]. The Chinese national standard has been set at 1 mg/L.

---

*Corresponding author.

However, more than 200 million people worldwide consume drinking water with a fluoride concentration higher than 1.0 mg/L [6]. Since a high concentration fluoride is detrimental to human health, fluoride removal from some drinking water source is a significantly important need.

Currently, many innovative techniques have been proposed to remove fluoride from drinking water. These techniques chiefly include adsorption, precipitation–coagulation, ion-exchange, membrane separation, electrolytic defluoridation and electrodialysis [7,8]. Among them, adsorption is considered to be one of the most effective methods to remove fluoride from drinking water and wastewater [6,9]. Various types of low-cost adsorbents, such as agricultural by-products, spent bleaching earth, bentonite and activated bentonite, wollastonite and chine clay, flax shive and biogas residual slurry, bone char, and zeolite, have been developed as new biosorbents [6,10–12]. However, the main disadvantages of these adsorbents are their lower adsorption efficiencies and narrow active pH ranges, which block their application in the treatment of drinking water [13]. Previous research on this new class of biosorbents is insufficient, and further study is essential.

Spent mushroom compost (SMC) is a lignocellulosic agricultural waste resulting from the cultivation and harvest mushroom crop. Each kilogram of harvest mushroom can generate approximately 5 kg of SMC [14]. In the European Union, the mushroom industry produces more than 3.5×10^6 tons of SMC every year [15]. This SMC is usually returned to fields as fertilizer or incinerated, the latter of which results in serious environmental pollution [16]. Thus, useful applications of SMC as an inexpensive lignocellulosic biomass have attracted much attention [14,16,17]. Thus far, little work has been done on the feasibility of use SMC derivatives to remove fluoride from aqueous solution such as drinking water.

Recent effort has been made to prepare new biosorbent using environmentally friendly biomass waste material. As a continuance of this work, we herein report the development of a new low-cost and highly effective biosorbent from SMC that efficiently removes fluoride from drinking water. The ability of coated spent mushroom compost biochar (SMCB) for the removal of fluoride from drinking water was evaluated. The dominant influencing factors, such as adsorbent dosage, contact time, initial concentration, pH, and coexisting ions were fully examined. The experimental data were modeled using several theoretical equations to adsorption efficiency. The use of a derivative of an agricultural waste to remove fluoride from drinking water is a win both for the environment and for human health.

2. Methods

2.1. Chemicals and materials

SMCB was provided by Huangshan University. Briefly, SMC was dried at 80˚C in a hot air oven for 8 h and then carbonized at 500˚C in an airtight muffle furnace for 2 h. SMCB was washed several times with distilled water to remove excess soluble salts and then was air-dried in a hot air oven at 100˚C for 5 h. Finally, the dried SMCB was ground into powder of mesh 60 and placed in an airtight container to obtain the initial SMCB sample (i.e., uncoated SMCB). All chemical reagents used in this work were analytical grade (AR), and all solutions were prepared in distilled water.

2.2. Preparation of the coated SMCB

The preparation of aluminum hydroxide-coated SMCB was similar to the technique reported by Ganvir and Das [18]. Briefly, 4.0 g SMCB and 40 mL aluminum sulfate solution were added to a beaker and stirred violently at 60˚C. The pH was then adjusted to 5.0 by the addition of a sodium hydroxide solution (five times the concentration of the aluminum sulfate solution). This solution was filtered by vacuum filtration and put into a hot air oven at 110˚C for 3 h to coat the SMCB with the aluminum hydroxide. To remove the sodium and sulfate salts, the coated SMCB was washed by distilled water several times and then air-dried in a hot air oven at 100˚C for 5 h. Finally, the coated SMCB was ground into powder of mesh 60 and placed in an airtight container.

2.3. Characterization of the samples

The specific surface area of initial SMCB and coated SMCB were determined by the BET method with N_2 gas using the automatic surface area analyzer (Tristar II 3020 M from Micromeritics). A scanning electron microscope (SEM, Sirion from FEI) was used to observe the surface images of the initial and coated SMCB. An energy-dispersive spectrometer (EDS, ESCALAB 250 from Thermo-VG Scientific) was used to analyze elemental composition of initial SMCB and coated SMCB surface. An X-ray powder diffractometer (XRD, X′ Pert PRO from PHILIPS) was used to analyze the structures and phases of initial SMCB and coated SMCB surface. The scanning rate was 8˚/min in the 2θ diffraction angle from 5˚ to 80˚.

2.4. Adsorption experiments and fluoride measurements

The adsorbent dosage (0.4–8.0 g/L), initial fluoride concentration (5–100 mg/L), contact time (1–960 min), pH (3.0–9.0), and the presence of co-ions (SO_4^{2-}, Cl^-, NO_3^-) were evaluated in a 50 mL centrifuge tube. The assay included 25 mL fluoride solution of known concentration. The pH of the solution was adjusted by 0.5 mol/L NaOH and HCl solution. The centrifuge tubes were kept at constant shaking (at 300 rpm) for 180 min at room temperature (25 ± 2℃) in a vapor-bathing constant temperature vibrator. The solution was separated by filtration. The fluoride ion concentration was measured (9609 BNWP fluoride ion selective electrode) following the method developed by Gao [19].

The amount of fluoride adsorbed per unit adsorbent (i.e., adsorption capacity, q_e) was calculated according to a mass balance on the fluoride concentration using Eq. (1).

$$q_e = \frac{V(C_0 - C_1)}{m} \tag{1}$$

where C_0 and C_1 are the initial and after-adsorption fluoride concentrations (mg/L), respectively, m is the dry weight of adsorbent (g), and V is the volume of fluoride solution (mL).

Each experiment was conducted three times, and adsorption capacity was expressed as the mean ± standard deviation.

3. Results and discussion

3.1. Characterization of initial SMCB and coated SMCB

The BET surface area of initial SMCB was found to be 3.6 m^2/g, while coated SMCB was 28.5 m^2/g. Since the surface areas of initial SMCB was much lower than commercial activated carbon (AC), aluminum hydroxide was coated onto SMCB to increase adsorption capacity, as surface area alone did not have a significant effect on the adsorption process. The data showed that the BET surface areas of the initial SMCB increased appreciably by the coating process. This increase in the surface areas could be assigned to the uniform coating of aluminum hydroxide (as amorphous precipitate of $Al(OH)_3$) on the surface of SMCB as reported by Tripathy et al. [9].

SEM image was used to analyze the surface texture and morphology of adsorbent. It could be observed in Fig. 1(a) that the initial SMCB had the expected plant structure and that the surface was smooth. However, from Fig. 1(b), it could be observed that some small particles of amorphous precipitate were present on the surface of the coated SMCB. This phenomenon could be attributed to the formation of an inorganic layer on the surface of SMCB as reported [13]. This presence of small particles on the surface of the coated SMCB greatly increased the surface area of the coated SMCB.

To further confirm the effective loading of aluminum hydroxide on the surface of SMCB, EDS spectra of the initial and coated samples were recorded. In the uncoated SMCB, the elemental peaks of carbon, oxygen, and calcium were observed (Fig. 1(c)). In the coated SMCB, a new peak of aluminum was observed besides the carbon and oxygen peaks (Fig. 1(d)), which shows that aluminum hydroxide is on the surface of the coated SMCB. This finding was consistent with conclusions reported by other authors. For example, Jain and Jayaram found signals corresponding to Al and O on aluminum hydroxide impregnated lime stone by energy-dispersive analysis of X-rays [20]. In addition, the intensity of the peak corresponding to calcium in the coated SMCB diminished. This may be due to loss of calcium salt during the coating process. Clearly, the results of EDS further corroborated the observations from the SEM images: That aluminum hydroxide was successfully coated on the surface of the SMCB.

For insight into the morphological nature of the aluminum hydroxide on the biochar, XRD patterns of the uncoated SMCB and coated SMCB were generated (Fig. 2). The XRD patterns of the SMCB (Fig. 2) showed intense peaks at 15˚, 24˚, 27˚, 30˚, and 38˚, which were characteristic of calcium salt and silicon dioxide. However, a strong peak was only detected at 27˚in the XRD pattern of the coated SMCB, which corresponds to the peak of silicon dioxide after being coated by aluminum hydroxide. No specific peak of alumina or aluminum hydroxide was observed in the XRD pattern of the coated SMCB. This finding indicated that aluminum hydroxide coated onto the SMCB surface was mainly amorphous. It is well known that amorphous materials have more active sites on their surfaces and a greater specific surface area allowing them to be used as good adsorbent [21]. Consequently, the coated SMCB was expected to be an efficient biosorbent for ions in solution.

3.2. Effect of aluminum sulfate concentration and pH on coating process

To study the effect of the aluminum sulfate concentration on the coating process, the concentrations of aluminum sulfate were varied from 0.2 to 0.7 mol/L. Adsorption capacity of the coated SMCB increased when the concentration of aluminum sulfate was increased from 0.2 to 0.3 mol/L (Fig. 3(a)). However, further increase in the concentration of aluminum sulfate hindered the aluminum hydroxide coating process [18]. As a result, adsorption capacity of the coated SMCB decreased when the concentration of aluminum

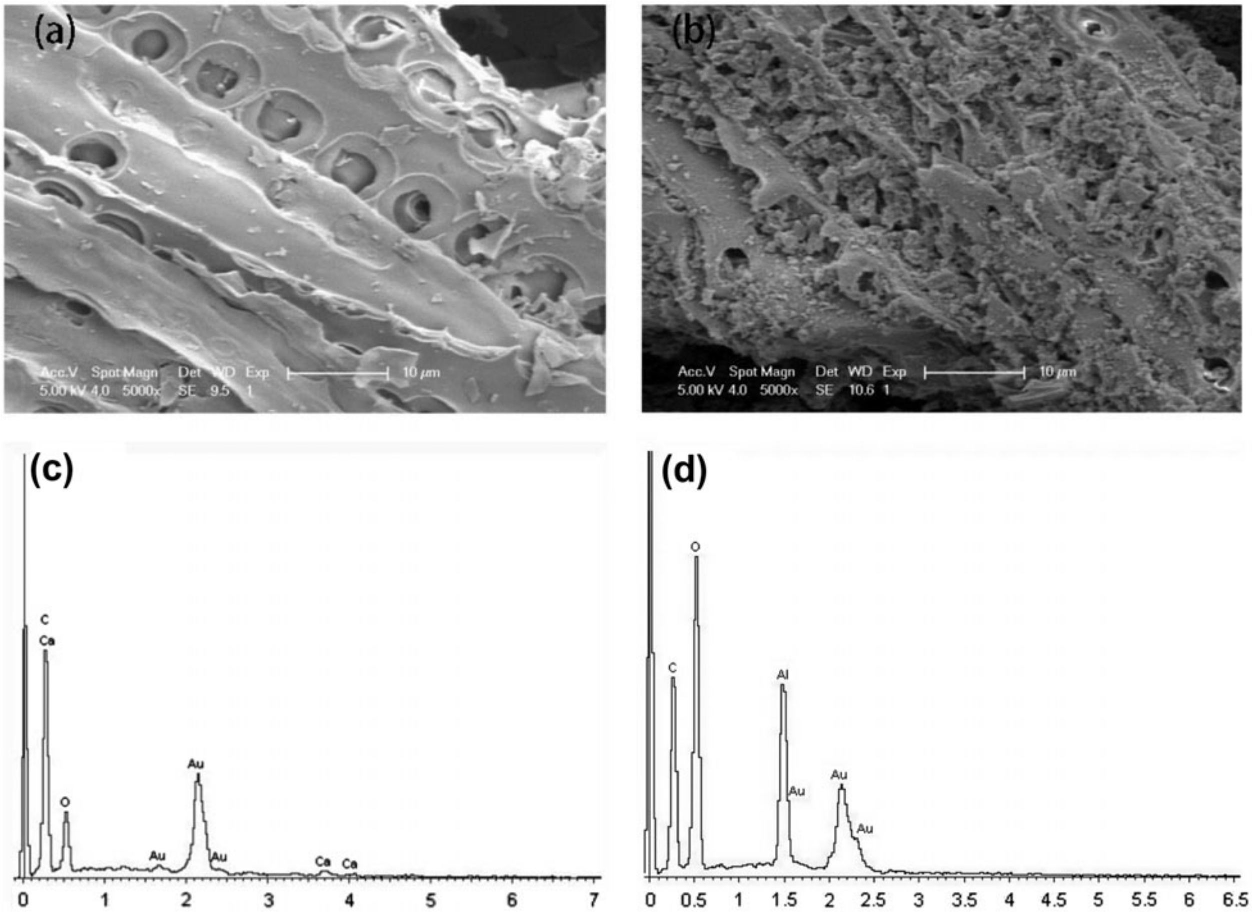

Fig. 1. SEM images of the uncoated SMCB (a) and the coated SMCB (b). EDS spectra of the uncoated SMCB (c) and the coated SMCB (d).

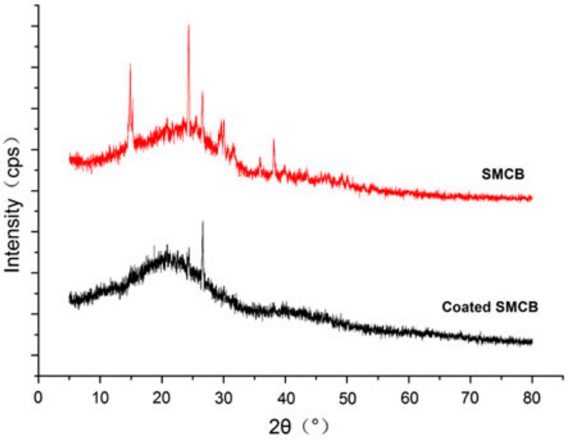

Fig. 2. XRD for the uncoated SMCB and the coated SMCB.

sulfate was greater than 0.3 mol/L. Thus, 0.3 mol/L aluminum sulfate was selected as the optimum concentration for coating the SMCB.

The impact of solution pH on the adsorption capacity of the coated SMCB was analyzed by varying the pH from 3.0 to 8.0 during the coating process. The fluoride removal capacity of the coated SMCB increased with an increase in pH, from 3.0 to 5.0 (Fig. 3(b)). The maximal adsorption value was achieved at pH 5.0. However, the fluoride removal capacity decreased when the pH exceeded 7.0. Since pH 5.0 was most suitable for fluoride removal, further coating processes were conducted at this pH.

3.3. Optimization of adsorption for fluoride removal

3.3.1. Determination of adsorbent dosage

The removal of fluoride ions by AC, activated alumina (AA), SMC, uncoated SMCB, and coated SMCB was compared under the same ranges of experimental conditions (Fig. 4). The coated SMCB exhibited a better performance than AC, AA, SMC, and SMCB for fluoride removal from aqueous solution.

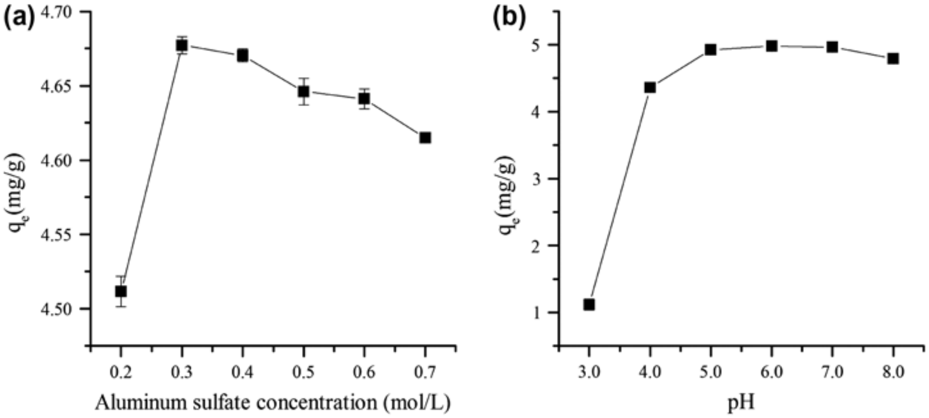

Fig. 3. Effect of aluminum sulfate concentration (a) and pH (b) on q_e of the coated SMCB.

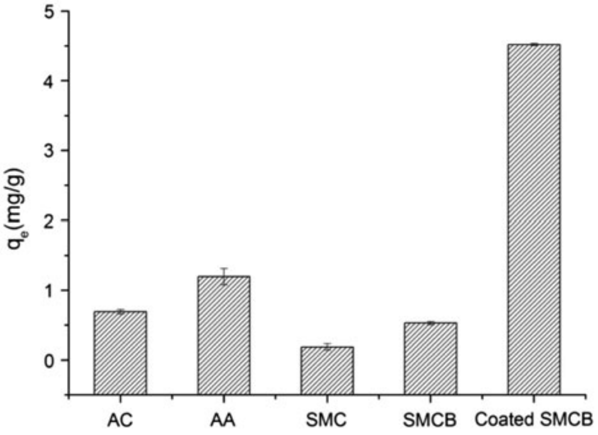

Fig. 4. The comparison of the coated SMCB for the removal of fluoride ions with activated carbon (AC), activated alumina (AA), SMC, and SMCB under the same ranges of experimental conditions (adsorbent 2 g/L, contact time 180 min, pH 7.0 ± 0.2, initial fluoride concentration 10 mg/L).

To gain insight into the effect of the adsorbent dosage on fluoride removal, a fluoride removal experiment was conducted at different dosages of uncoated and coated SMCB (0.4, 0.8, 2.0, 4.0, 6.0, and 8.0 g/L; Fig. 5(a)). The native SMCB had poor fluoride adsorption. On the other hand, the percentage of fluoride removed by the coated SMCB increased as the dosage of adsorbent rose from 0.4 to 8.0 g/L. In contrast, the adsorption capacity of fluoride indicated an opposite trend. Two dominating factors might be responsible: (1) The aggregation of adsorbent particles at high dosages may lead to an increase in the diffusional path length and a decrease in surface area; or (2) the diminishing number of adsorption sites remaining unsaturated during the adsorption process leads to a drop in the adsorption capacity as the adsorbent dosages increased, similar to results reported by Daifullah [11]. It should be emphasized that there was only a slight improvement in the removal of fluoride when the adsorbent dosage was above 2.0 g/L and the concentration of fluoride after adsorption was under the Chinese national standard in drinking water (1 mg/L). Therefore, the minimum adsorbent dosage for maximum fluoride removal was set at 2.0 g/L, which was used as the optimum dosage for further experiments.

3.3.2. Contact time vs. adsorption capacity

The relationship between the fluoride adsorption capacity (q_t, mg/g) and contact time (t, min) was measured (Fig. 5(b)) demonstrates that the adsorption of fluoride on the coated SMCB increased rapidly in the first ten minutes. Subsequently, the adsorption increased slowly and reached the equilibrium state as the contact time passed 180 min. The fast adsorption rate at the initial stage might be attributable to the participation of active surface sites and specific functional groups [22]. Similar equilibrium time was obtained for the adsorption of fluoride on $KMnO_4$-modified AC [11]. Consequently, adsorption experiments were performed for 180 min to ensure that the equilibrium state was completely reached.

3.3.3. The initial concentration of fluoride vs. adsorption capacity

The effect of the initial concentration of fluoride on the adsorption capacity was investigated by varying the concentration of fluoride solutions from 5 to 100 mg/L (Fig. 5(c)). According to the results, the

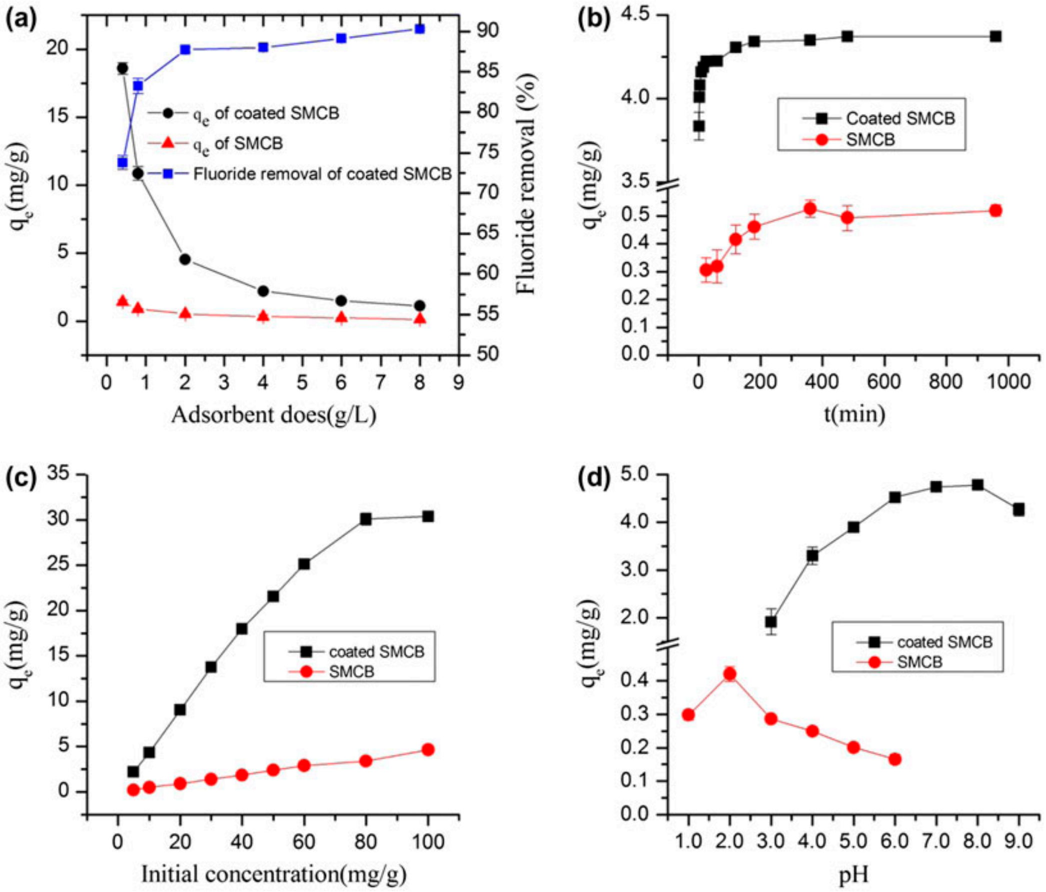

Fig. 5. Effect of the adsorbent dosage (a), contact time (b), initial fluoride concentration (c), and pH (d) on the q_e of the uncoated SMCB and the coated SMCB.

coated SMCB had a much higher fluoride adsorption capability than the uncoated SMCB. Furthermore, the fluoride adsorption capacity of the coated SMCB increased rapidly and then reached a plateau as the initial concentration of fluoride increased (Fig. 5(c)), suggesting that the adsorption capacity increased with an increase in the initial concentration of fluoride. The ratio of surface active sites to the total fluoride might be responsible for such trend. At low fluoride concentrations, the fluoride ions moved easily to the surface active sites; thus, the fluoride ions could interact with the adsorbent to occupy the active sites on the surface of the coated SMCB and be sufficiently removed from solution. However, at a high concentration of fluoride, not all fluoride ions could easily arrive at the surface active sites, and the number of active sites was not enough to accommodate the number of fluoride ions. This would thus result in lower adsorption capacity of fluoride [23]. The results suggested that the equilibrium concentration of fluoride in drinking water could be reduced to a level of 1 mg/L under the current experimental conditions, when the initial fluoride concentration was below 10 mg/L.

3.3.4. *pH of aqueous solution vs. adsorption capacity*

The effect of pH on the adsorption capacity of fluoride on the coated SMCB was studied by varying the pH ranges from 3.0 to 9.0 (Fig. 5(d)). The fluoride adsorption capacity of the uncoated SMCB and the coated SMCB was highly dependent on pH. It was evident that the coating process created much higher fluoride adsorption capacity for the SMCB. The adsorption capacity of fluoride on the coated SMCB increased with increasing pH of the solution and reached a maximum (*ca*. 4.7 mg/g) at pH 7.0. The adsorption capacity decreased dramatically when the pH was higher than 8.0. This finding was consistent with the results obtained by other researchers [10,24].

To explain the above trend, the formation of the fluoride complex should be examined. At lower pH, fluoride ions easily combined with aluminum hydroxide to form AlF_x species in solution; this would thus decrease the adsorption capacity for fluoride. However, at too high a pH, OH^- would be displaced by F^- from the coated SMCB, and the number of F^- adsorbed or converted to complexes would decline rapidly [7], leading to a larger decrease in adsorption capacity. These results suggested that the pH of the solution played an important role in the removal of fluoride, with a wide optimum pH range of 6.0–8.0. The adsorption mechanism could be proposed as follows.

Aluminum ions have an affinity for fluoride ions, a hard–hard interaction that also follows the soft–hard acid base concept proposed by Tchomgui-Kamga et al. [13]. Therefore, aluminum compounds are usually used to defluorinate aqueous solutions. The mechanism for fluoride adsorption by aluminum hydroxide under acidic conditions can be represented schematically as follows [25]:

$$\equiv \mathrm{MOH} + \mathrm{H}^+ \leftrightarrow \equiv\ \mathrm{MOH}_2^+ \tag{2}$$

$$\equiv \mathrm{MOH}_2^+ + \mathrm{F}^- \leftrightarrow \equiv\ \mathrm{MF} + \mathrm{H_2O} \tag{3}$$

Fluoride is adsorbed predominantly by the following mechanism at $pH > 6$.

$$\equiv \mathrm{MOH} + \mathrm{F}^- \leftrightarrow \equiv\ \mathrm{MF} + \mathrm{HO}^- \tag{4}$$

where M represents metal ion (Al in this case), and MOH and MF represent a surface hydroxyl group and a surface site occupied by a fluoride ion, respectively.

To our knowledge, the dispersion of aluminum hydroxide on the surface of SMCB has never been studied. We followed the hypothesis that a nanoscale dispersion of the inorganic adsorbent on the surface of the coated SMCB might be an interesting way to generate an efficient fluoride scavenger. The results showed that the coated SMCB was more effective than reported biomass-based adsorbents. Therefore, adsorbents coated by aluminum hydroxide would be new and efficient biosorbent.

3.3.5. The effect of coexisting ions in fluoride aqueous solution on fluoride adsorption

Drinking water usually contains other anions in addition to fluoride, which may affect the removal of fluoride. The effect of coexisting ions on fluoride adsorption was investigated and (Fig. 6). The concentration of each anion (SO_4^{2-}, Cl^-, NO_3^-) varied from 50 to 200 mg/L with a fixed fluoride concentration of 10 mg/L (Fig. 6). The effect of both chloride and nitrate on the defluoridation capacity of adsorbents was negligible within the context of all coexisting ions, which was consistent with previous conclusions [3,26]. In contrast, sulfate ions displayed a minor interference (causing a decrease below 10%). This has been partly attributed to its higher negative charge [11,26]. Based on these findings, it could be reasoned that the concentration of SO_4^{2-}, Cl^- and NO_3^- did not have a significant effect on the defluoridation yield even if their amounts in solution were elevated to a higher level. This high affinity and selectivity for fluoride adsorption made the coated SMCB a suitable biosorbent for the treatment of fluoride-containing water.

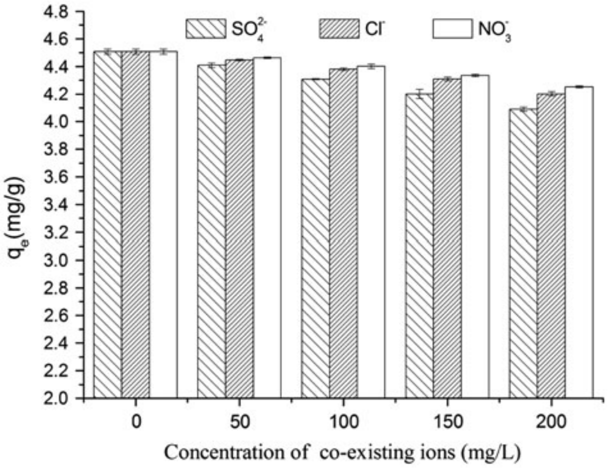

Fig. 6. Effect of the coexisting ions on the q_e of the coated SMCB.

3.4. Adsorption isotherms

The sorption isotherm expresses the specific relationship between the degree of accumulation on the adsorbent surface and the concentration of sorbate at constant temperature [27]. To study the adsorption behavior of fluoride on the coated SMCB, the experimental data were analyzed using Langmuir and Freundlich isotherm models.

The Langmuir isotherm model, which is valid for monolayer adsorption with uniform energies of adsorption, was represented in Eq. (5):

$$\frac{c_e}{q_e} = \frac{1}{q_0 b} + \frac{c_e}{q_0} \tag{5}$$

where C_e (mg/L) and q_e (mg/L) are the concentration and adsorption capacity at equilibrium, respectively,

b (L/mg) is the adsorption equilibrium constant that relates to the adsorption energy, and q_0 (mg/g) is the amount of the fluoride ion per weight of coated SMCB, which estimates the maximum uptake of adsorbent. The values of q_0 and b can be calculated from the slops and intercept of the plot of C_e/q_e vs. C_e. The corresponding results were presented in Fig. 7(a).

The Freundlich isotherm model is expressed as follows:

$$\lg q_e = \lg k + \frac{1}{n}\lg c_e \tag{6}$$

where k and $1/n$ represent adsorption capacity and adsorption intensity, respectively, and can be calculated from the intercept and the slope of the straight line for the lg–lg plot of q_e and vs. C_e. The obtained results were given in Fig. 7(b).

The parameter values obtained from the Langmuir and Freundlich isotherms are listed in Table 1. It could be seen that the experimental data better fit the Langmuir isotherm model ($R^2 = 0.9579$). However, the data did not fit the Freundlich isotherm model well ($R^2 = 0.8010$). This finding indicated that the adsorption of fluoride on the surface of coated SMCB was a monolayer process, which was consistent with the results reported by Tchomgui-Kamga et al. [13]. Moreover, it could be seen that the maximum adsorption capacity of fluoride is theoretically 36.5 mg/g.

3.5. Adsorption kinetics

Lagergern adsorption kinetics is a helpful tool to predict the adsorption rate and understand the mechanism of fluoride adsorption. Typically, Lagergern pseudo-first-order and pseudo-second-order kinetic models can be linearly expressed as Eqs. (7) and (8).

$$\log(q_e - q_t) = \log q_e - \frac{k_1}{2.303}t \tag{7}$$

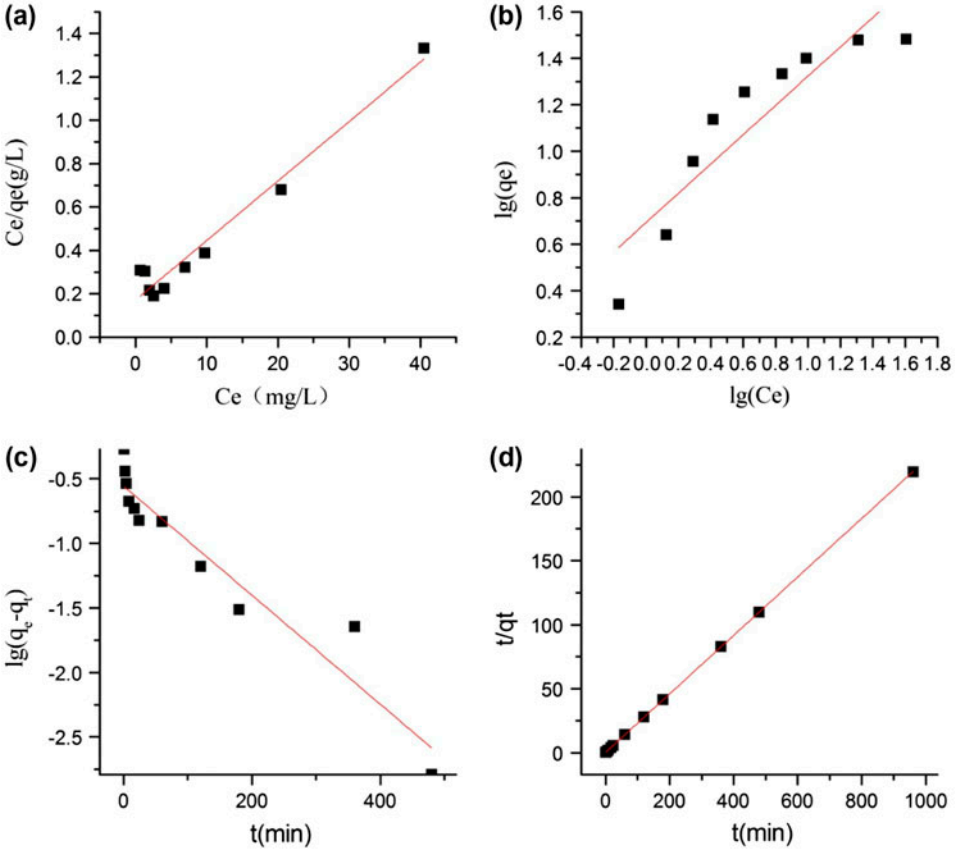

Fig. 7. Langmuir isotherm (a) and Freundlich isotherm (b), the pseudo-first-order kinetic model (c), and the pseudo-second-order kinetic model (d) for fluoride adsorption on the coated SMCB.

Table 1
Langmuir and Freundlich isotherm constants for adsorption of fluoride on the coated SMCB

Langmuir isotherm			Freundlich isotherm		
q_0 (mg/g)	b (L/mg)	R^2	n	K (mg/g)	R^2
36.47	0.1598	0.9579	1.588	4.501	0.8010

or,

$$\frac{t}{q_t} = \frac{1}{k_2 q_e^2} + \frac{1}{q_e} t \tag{8}$$

where k_1 and k_2 are the rate constants of pseudo-first-order and pseudo-second-order kinetic models, respectively, and q_t and q_e are the amount of adsorbed fluoride at any time and at equilibrium state (mg/g), respectively.

The parameter values obtained from Lagergern pseudo-first-order and pseudo-second-order kinetic models are listed in Table 2. These data demonstrated that the linear regression coefficient ($R^2 = 0.8275$) of Lagergern pseudo-first-order model for fluoride adsorption indicated a poor fit (Fig. 7(c)).

However, the linear regression coefficient (R^2) of the Lagergern pseudo-second-order model for fluoride adsorption has a better fit, $R^2 = 0.9999$ (Fig. 7(d)) indicating that fluoride adsorption on the coated SMCB followed the Lagergern pseudo-second-order kinetics model. Furthermore, it could be seen that the calculated equilibrium adsorption capacity q_e was equal to 4.8 mg/g, which was close to the experimental capacity (4.7 mg/g). These results suggested that the adsorption of fluoride on the coated SMCB might be dominated by chemical adsorption. This reason could be due to valence forces that occur as a result of exchanging or sharing electrons between the adsorbent and anions [28]. Similar results were also found for the adsorption of fluoride on various other adsorbents [18].

3.6. Comparison of adsorption capacity with those obtained in other biomass-based adsorbents

To access the removal efficiency of fluoride by the coated SMCB, the maximum adsorption capacity in this case was compared with those obtained in some biomass-based adsorbents reported in the literature (Table 3). The coated SMCB exhibited considerably higher adsorption capacity for fluoride ions than other biomass-based adsorbents. Although the adsorption capacity of fluoride on the coated SMCB was lower than that of the zirconium ion-impregnated coconut fiber carbon, fluoride adsorption on the coated SMCB was more rapid. In particular, zirconium ion-impregnated

Table 2
Lagergern pseudo-first-order and pseudo-second-order kinetic models constants for adsorption of fluoride on the coated SMCB

	The pseudo-first-order kinetic model			The pseudo-second-order kinetic model		
Experimental capacity (mg/g)	k_1 (1/min)	q_e (mg/g)	R^2	k_2 (g/mg min)	q_e (mg/g)	R^2
4.7	327.3	4.4	0.8275	0.1891	4.8	0.9999

Table 3
Comparison of adsorption capacity of fluoride on the coated SMCB with those reported in references

Sorbent	q_0 (mg/g)	pH	Contact time (h)	Reference
Zirconium ion-impregnated coconut fiber carbon	40.0	4.0	6	[29]
Zr(IV)-loaded dried orange juice residue	27.17	4.0	4	[10]
Fe(III)-loaded cotton cellulose	18.6	4.0–9.0	8	[30]
Aluminum-impregnated hierarchal web of carbon fibers	17.0	–	–	[31]
$KMnO_4$-modified activated carbon from rice straw	15.9	2.0	3	[11]
Aluminum hydroxide-coated rice husk ash	15.0	7.0	1	[18]
Charcoals contain dispersed aluminum oxide	13.6	7.0	8	[13]
Waste carbon slurry	4.3	7.6	1	[32]
Wheat straw raw	1.9	6.0	1	[6]
SMCB coated by aluminum hydroxide	36.5	6.0–8.0	3	This work

coconut fiber carbon adsorption was mainly based on a technology for fluoride removal in acidic solution, which is not a feasible condition for application to rural areas. In contrast, the coated SMCB technique should overcome such a demerit. The coated SMCB can be used over wide a pH range, which will provide great operational advantages and can be easily achieved in rural environments. Furthermore, the SMC is easily available free of cost from mushroom farms. The cost of consumables and the preparation price are similar to those of other biomass-based adsorbents [33]. Consequently, coated SMCB is a desirable biosorbent for fluoride removal from water.

4. Conclusions

In this study, a low-cost biosorbent, derived from SMC, was prepared with aluminum hurried and tested for adsorption of fluoride. The fluoride adsorption capacity from drinking water was as high as of 4.7 mg/g under optimum condition (pH 7.0, 3.0 h contact time, and adsorbent dosage of 2.0 g/L) from an aqueous solution of 10 mg/g fluoride. In addition, coexisting ions had little effect on the defluoridation yield, but solution pH played an important role in the removal of fluoride from water.

Acknowledgments

Financial supports from the Earmarked Fund for Modern Agro-industry Technology Research System in Tea Industry (CARS-23, the Ministry of Agriculture of P.R. China) and Natural Science Foundation of Anhui Province (1408085MKL38) are highly appreciated. The authors thank Huangshan University for providing SMCB samples and the teachers of University of Science and Technology of China for characterizing the sample.

References

[1] C.K. Geethamani, S.T. Ramesh, R. Gandhimathi, P.V. Nidheesh, Alkali-treated fly ash for the removal of fluoride from aqueous solutions, Desalin. Water Treat. 52 (2014) 3466–3476.
[2] H.T. Dean, F.A. Arnold Jr., P. Jay, J.W. Knutson, Studies on mass control of dental caries through fluoridation of the public water supply, Public Health Rep. 65 (1950) 1403–1408.
[3] T. Zhang, Q.R. Li, Z.Y. Mei, H.Y. Xiao, H.X. Lu, Y.M. Zhou, Adsorption of fluoride ions onto non-thermal plasma-modified CeO_2/Al_2O_3 composites, Desalin. Water Treat. 52 (2014) 3367–3376.
[4] K. Sarala, P.R. Rao, Endemic fluoride in the village Ralla, Anantapuram in Andhra Pradesh—An epidemiological study, Fluoride 26 (1993) 177–180.
[5] World Health Organization, Guidelines for Drinking Water Quality, WHO, Geneva, Switzerland, 1993.
[6] A.K. Yadav, R. Abbassi, A. Gupta, M. Dadashzadeh, Removal of fluoride from aqueous solution and groundwater by wheat straw, sawdust and activated bagasse carbon of sugarcane, Ecol. Eng. 52 (2013) 211–218.
[7] A. Bhatnagar, E. Kumar, M. Sillanpää, Fluoride removal from water by adsorption—A review, Chem. Eng. J. 171 (2011) 811–840.
[8] D. Ghosh, M.K. Sinha, M.K. Purkait, A comparative analysis of low-cost ceramic membrane preparation for effective fluoride removal using hybrid technique, Desalination 327 (2013) 2–13.
[9] S.S. Tripathy, J.L. Bersillon, K. Gopal, Removal of fluoride from drinking water by adsorption onto alum-impregnated activated alumina, Sep. Purif. Technol. 50 (2006) 310–317.
[10] H. Paudyal, B. Pangeni, K. Inoue, H. Kawakita, K. Ohto, K.N. Ghimire, H. Harada, S. Alam, Adsorptive removal of trace concentration of fluoride ion from water using dried orange juice residue, Chem. Eng. J. 223 (2013) 844–853.
[11] A.A.M. Daifullah, S.M. Yakout, S.A. Elreefy, Adsorption of fluoride in aqueous solutions using $KMnO_4$-modified activated carbon derived from steam pyrolysis of rice straw, J. Hazard. Mater. 147 (2007) 633–643.
[12] Y.B. Sun, Q.H. Fang, J.P. Dong, X.W. Cheng, J.Q. Xu, Removal of fluoride from drinking water by natural stilbite zeolite modified with Fe(III), Desalination 277 (2011) 121–127.
[13] E. Tchomgui-Kamga, V. Alonzo, C.P. Nanseu-Njiki, N. Audebrand, E. Ngameni, A. Darchen, Preparation and characterization of charcoals that contain dispersed aluminum oxide as adsorbents for removal of fluoride from drinking water, Carbon 48 (2010) 333–343.
[14] K.N. Finney, C. Ryu, V.N. Sharifi, J. Swithenbank, The reuse of spent mushroom compost and coal tailings for energy recovery: Comparison of thermal treatment technologies, Bioresour. Technol. 100 (2009) 310–315.
[15] F.J. Gea, M. Santos, F. Diánez, J.C. Tello, M.J. Navarro, Effect of spent mushroom compost tea on mycelial growth and yield of button mushroom (*Agaricus bisporus*), World J. Microb. Biotechnol. 28 (2012) 2765–2769.
[16] A. Abu Bakar, N.Z. Mahmood, J.A.T. da Silva, N. Abdullah, A.A. Jamaluludin, Vermicomposting of sewage sludge by *Lumbricus rubellus* using spent mushroom compost as feed material: Effect on concentration of heavy metals, Biotechnol. Bioprocess Eng. 16 (2011) 1036–1043.
[17] Y. Kwack, J.H. Song, Y. Shinohara, T. Maruo, C. Chun, Comparison of six spent mushroom composts as growing media for transplant production of lettuce, Compost Sci. Util. 20 (2012) 92–96.
[18] V. Ganvir, K. Das, Removal of fluoride from drinking water using aluminum hydroxide coated rice husk ash, J. Hazard. Mater. 185 (2011) 1287–1294.
[19] H.J. Gao, Z.Z. Zhang, X.C. Wan, Influences of charcoal and bamboo charcoal amendment on soil–fluoride fractions and bioaccumulation of fluoride in tea plants, Environ. Geochem. Health 34 (2012) 551–562.
[20] S. Jain, R.V. Jayaram, Removal of fluoride from contaminated drinking water using unmodified and

aluminium hydroxide impregnated blue lime stone waste, Sep. Sci. Technol. 44 (2009) 1436–1451.

[21] G.S. Zhang, J.H. Qu, H.J. Liu, R.P. Liu, R.C. Wu, Preparation and evaluation of a novel Fe–Mn binary oxide adsorbent for effective arsenite removal, Water Res. 41 (2007) 1921–1928.

[22] S.V. Mohan, J. Karthikeyan, Removal of lignin and tannin colour from aqueous solution by adsorption onto activated charcoal, Environ. Pollut. 97 (1997) 183–187.

[23] S.F. Montanher, E.A. Oliveira, M.C. Rollemberg, Removal of metal ions from aqueous solutions by sorption onto rice bran, J. Hazard. Mater. 117 (2005) 207–211.20. 21. 22.

[24] S. Ghorai, K.K. Pant, Equilibrium, kinetics and breakthrough studies for adsorption of fluoride on activated alumina, Sep. Purif. Technol. 42 (2005) 265–271.

[25] M.G. Sujana, G. Soma, N. Vasumathi, S. Anand, Studies on fluoride adsorption capacities of amorphous Fe/Al mixed hydroxides from aqueous solutions, J. Fluorine Chem. 130 (2009) 749–754.

[26] X.H. Wang, R.H. Song, H.C. Yang, Y.J. Shi, G.B. Dang, S. Yang, Y. Zhao, X.F. Sun, S.G. Wang, Fluoride adsorption on carboxylated aerobic granules containing Ce(III), Bioresour. Technol. 127 (2013) 106–111.

[27] G. Alagumuthu, M. Rajan, Equilibrium and kinetics of adsorption of fluoride onto zirconium impregnated cashew nut shell carbon, Chem. Eng. J. 158 (2010) 451–457.

[28] C. Duran, D. Ozdes, A. Gundogdu, H.B. Senturk, Kinetics and isotherm analysis of basic dyes adsorption onto almond shell (*Prunus dulcis*) as a low cost adsorbent, J. Chem. Eng. Data 56 (2011) 2136–2147.

[29] R.S. Sathish, S. Sairam, V.G. Raja, G.N. Rao, C. Janardhana, Defluoridation of water using zirconium impregnated coconut fiber carbon, Sep. Sci. Technol. 43 (2008) 3676–3694.

[30] Y.P. Zhao, X.Y. Li, L. Liu, F.H. Chen, Fluoride removal by Fe(III)-loaded ligand exchange cotton cellulose adsorbent from drinking water, Carbohydr. Polym. 72 (2008) 144–150.

[31] A.K. Gupta, D. Deva, A. Sharma, N. Verma, Adsorptive removal of fluoride by micro-nanohierarchal web of activated carbon fibers, Ind. Eng. Chem. Res. 48 (2009) 9697–9707.

[32] V.K. Gupta, I. Ali, V.K. Saini, Defluoridation of wastewaters using waste carbon slurry, Water Res. 41 (2007) 3307–3316.

[33] H.M. Cai, G.J. Chen, C.Y. Peng, Z.Z. Zhang, Y.Y. Dong, G.Z. Shang, X.H. Zhu, H.J. Gao, X.C. Wan, Removal of fluoride from drinking water using tea waste loaded with Al/Fe oxides: A novel, safe and efficient biosorbent, Appl. Surf. Sci. 328 (2015) 34–44.